Modeling of the general astigmatic Gaussian beam and its propagation through 3D optical systems

Evgenia Kochkina,[1,2,*] Gudrun Wanner,[1,2] Dennis Schmelzer,[1,2]
Michael Tröbs,[1,2] and Gerhard Heinzel[1,2,3]

[1]Max Planck Institute for Gravitational Physics (Albert Einstein Institute), Callinstr. 38, D-30167, Hannover, Germany

[2]QUEST Centre of Quantum Engineering and Space-Time Research, Leibniz University of Hannover,
Hannover, Germany

[3]e-mail: gerhard.heinzel@aei.mpg.de

*Corresponding author: evgenia.kochkina@aei.mpg.de

The paper introduces the complete model of the general astigmatic Gaussian beam as the most general case of the Gaussian beam in the fundamental mode. This includes the laws of propagation, reflection, and refraction as well as the equations for extracting from the complex-valued beam description its real-valued parameters, such as the beam spot radii and the radii of curvature of the wavefront. The suggested model is applicable to the case of an oblique incidence of the beam at any 3D surface that can be approximated by the second-order equation at the point of incidence. Thus it can be used in simulations of a large variety of 3D optical systems. The provided experimental validation of the model shows good agreement with simulations. © 2013 Optical Society of America

OCIS codes: (140.3295) Laser beam characterization; (000.3860) Mathematical methods in physics; (080.2468) First-order optics; (350.5500) Propagation.

http://dx.doi.org/10.1364/AO.52.006030

1. Introduction

The propagation of stigmatic Gaussian beams through rotationally symmetric optical systems can be described by well-known laws [1]. Such beams have circular light spots and spherical (or flat) wavefronts at every point along the optical path. The symmetry might be broken, for example, when a Gaussian beam impinges on a curved surface at an oblique angle. After such a transformation the beam becomes simple (or orthogonal) astigmatic [2] with elliptical light spots and ellipsoidal or hyperboloidal wavefronts [3]. For brevity we will denote all non-spherical wavefronts as ellipsoidal in the following sections. The representation of the simple astigmatic beam can be split into two independent circular

Gaussian beam representations, which means that the conventional laws [1] are still applicable in this case. The ellipses of constant intensity and of constant phase are aligned and their orientation stays constant at every point along the beam path. Therefore, a simple astigmatic Gaussian beam has two principal directions in the transversal plane and thus can be called elliptical. This model requires the optical system to be orthogonal. In such a system, for any beam transformation at a surface two restrictions have to be fulfilled: (1) one of the principal directions of the beam must lie in the plane of incidence (the plane defined by the beam axis and the normal to the surface at the point of incidence); (2) one of the principal axes of the surface must lie in the plane of incidence. The second restriction can never be violated in the case of plane or spherical surfaces. Unfortunately, this is not true for the first restriction. As discussed above, the simple astigmatic beam can

be obtained via refraction of a circular beam at a spherical surface. Let this simple astigmatic beam pass through another spherical surface such that the plane of incidence at this surface is not equal or orthogonal to the plane of incidence at the first surface (see Fig. 1). In this case, none of the principal axes of the beam ellipse lies in the plane of incidence, and it becomes impossible to decompose the behavior of the resulting beam into two orthogonal planes. The outgoing beam becomes generally astigmatic [4], with an ellipse of constant intensity and an ellipse of constant phase oriented at an oblique angle with respect to each other. The phase ellipse of the outgoing beam is rotated with respect to the phase ellipse of the incident beam, while the intensity ellipse stays unaffected. Moreover, the orientations of both ellipses, as well as their relative orientation, change along the propagation. These properties are even easier to observe if the general astigmatic beam is obtained by tracing a stigmatic Gaussian beam through two cylindrical lenses oriented at an oblique angle with respect to each other. However, we do stress that even an optical system that consists exclusively of rotationally symmetric components can transform stigmatic Gaussian beams into general astigmatic beams. In many cases, after such transformation, both ellipses of constant intensity and of constant phase have small ellipticity, which allows the use of the simple astigmatic or even circular Gaussian beam approximation. However, when designing high-precision instruments the difference might not be negligible.

A general astigmatic Gaussian beam is the most general case of the Gaussian beam in the fundamental mode. Simple astigmatic and circular beams can be treated as special cases of the general astigmatic beam. Therefore, any general astigmatic Gaussian beam model can be thought of as a model of the arbitrary Gaussian beam in the fundamental mode. The conventional laws [1] are not applicable to general astigmatic Gaussian beams. The complete description of their propagation in free space is given

in [4]. Unfortunately, this study provides limited possibilities for beam transformation and does not include the case of nonnormal incidence. To our knowledge, the only work so far that can transform astigmatic beams incident at some angle on an arbitrary second-order surface (for example a sphere, ellipsoid or cylinder), is [5]. However, due to the typos, one needs to rederive the formulas from this paper in order to use them.

In our paper, we will present the complete general astigmatic Gaussian beam model. To our knowledge, this is the first description of general astigmatic beams that includes all aspects necessary for simulation of their propagation in an arbitrary optical system. In this paper we will not only summarize the previously available investigations, but also correct the typos and generalize the beam transformation equations from [5] to avoid restrictions in the choice of beam-fixed and surface-fixed coordinate systems. The important advantage of the suggested model is that it allows the study of the effects of simple and general astigmatism, even when they are small and considered to be negligible by most other models. This can happen, for example, when the optical system is slightly misaligned or the incidence is close to normal. This model is implemented in the software tool IFOCAD [6] and can be used to compute the interferometer signals described in [7].

In Section 2 we discuss the mathematical description of general astigmatic Gaussian beams, including the complex radius of curvature tensor [8] and the complex amplitude. Section 3 introduces the physical interpretation of these complex-valued parameters. Section 4 includes the laws of reflection and refraction of the general astigmatic Gaussian beam. In the last section, we present the results of the experimental verification of the suggested model.
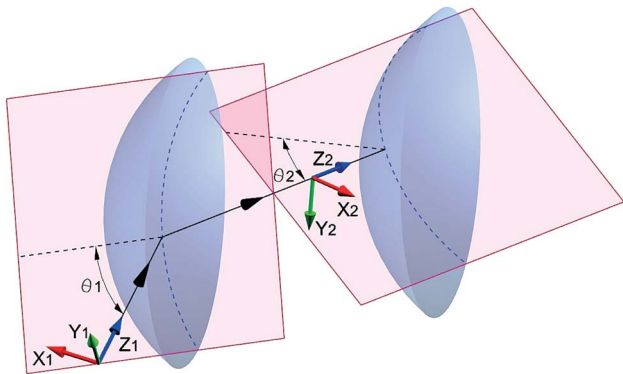

Fig. 1. Nonorthogonal optical system consisting of the two spherical lenses. The plane of incidence for the beam transformation by the first lens and the plane of incidence for the beam transformation by the second lens are aligned at an oblique angle with respect to one other.

2. Mathematical Description of the General Astigmatic Gaussian Beam

The complex amplitude describing simple astigmatic beam propagation along the z axis, written in its principal coordinate system, is [4,7]

$$E(x, y, z)$$
$$= E_0(z) \exp\left[-i\phi_{ac} + i\eta(z) - i\frac{k}{2}\left(\frac{x^2}{q_x(z)} + \frac{y^2}{q_y(z)}\right)\right], \quad (1)$$

where $k = 2\pi/\lambda$ is the wavenumber, λ is the optical wavelength in the medium, and q_x and q_y are the q-parameters of the beam,

$$q_{x,y} = 1/R_{x,y} - i\lambda/(\pi w_{x,y}^2), \quad (2)$$

with $w_{x,y}$ being the principal semi-axes of the spot ellipse and $R_{x,y}$ being the principal semi-axes of the phase ellipse. The accumulated phase ϕ_{ac} is defined as

$$\phi_{ac} = \sum_j k_j l_j, \qquad (3)$$

where k_j is the wavenumber and l_j is the geometrical distance in each of the media that the beam is propagated through from the chosen reference point. The term $\eta(z)$ is a Gouy phase shift (see [9] for an example) and it is defined as follows [4]:

$$\eta(z) = \frac{1}{2}\left[\arctan\left(\frac{\Re(q_x)}{\Im(q_x)}\right) + \arctan\left(\frac{\Re(q_y)}{\Im(q_y)}\right)\right]. \qquad (4)$$

$\Re(q)$ and $\Im(q)$ stand for the real and imaginary parts of the complex number q, respectively.

By rotating the beam ellipse counterclockwise around the z axis by an angle of θ with respect to the global coordinate system (x,y,z) we obtain

$$\begin{aligned}
E(x,y,z) = E_0(z)\exp\Bigg\{&-i\phi_{ac} + i\eta(z) \\
&- i\frac{k}{2}\Bigg[\left(\frac{\cos^2\theta}{q_1(z)} + \frac{\sin^2\theta}{q_2(z)}\right)x^2 \\
&+ \left(\frac{\sin^2\theta}{q_1(z)} + \frac{\cos^2\theta}{q_2(z)}\right)y^2 \\
&+ \sin 2\theta\left(\frac{1}{q_1(z)} - \frac{1}{q_2(z)}\right)xy\Bigg]\Bigg\}.
\end{aligned} \qquad (5)$$

Here, we no longer use the indices x and y for q-parameters, to emphasize that they do not correspond to the x and y axes any longer.

If, instead, we rotated the coordinate system (x,y,z) counterclockwise with respect to the principal coordinate system of the beam, the coefficient of the xy term in Eq. (5) would have the opposite sign (see [4] for an example).

The complex amplitude of the general astigmatic beam is the same as the complex amplitude of the simple astigmatic beam tilted around the axis of propagation (z axis) by an angle of θ [Eq. (5)], with the only difference being that this angle is now complex [4]. The Gouy phase for the general astigmatic beam is defined using the same equation as for the simple astigmatic beam [Eq. (4)] [4].

Equation (5) can be rewritten as

$$E(\mathbf{r},z) = E_0(z)\exp\left\{-i\phi_{ac} + i\eta(z) - i\frac{k}{2}\mathbf{r}^T Q(z)\mathbf{r}\right\}, \qquad (6)$$

where

$$Q(z) = \begin{pmatrix} \frac{\cos^2\theta}{q_1(z)} + \frac{\sin^2\theta}{q_2(z)} & \frac{1}{2}\sin 2\theta\left(\frac{1}{q_1(z)} - \frac{1}{q_2(z)}\right) \\ \frac{1}{2}\sin 2\theta\left(\frac{1}{q_1(z)} - \frac{1}{q_2(z)}\right) & \frac{\sin^2\theta}{q_1(z)} + \frac{\cos^2\theta}{q_2(z)} \end{pmatrix} \qquad (7)$$

is the complex radius of curvature tensor for generalized Gaussian beams [8], $\mathbf{r} = (x,y)^T$ is a vector of transversal coordinates, and the superscript T stands for transposed.

The complex-valued expression in the exponent of Eq. (6) is a complex phase,

$$\phi(\mathbf{r},z) = -i\phi_{ac} + i\eta(z) - i\frac{k}{2}\mathbf{r}^T Q(z)\mathbf{r}. \qquad (8)$$

In [10] the simple analytic formula that describes the propagation of a general astigmatic Gaussian beam in a homogeneous medium is given by

$$Q' = \frac{Q}{I_2 + \Delta z Q}, \qquad (9)$$

where I_2 is the unit matrix of size two and Δz is the propagation distance. Equation (9) is equivalent to

$$Q' = \begin{pmatrix} \frac{\cos^2\theta}{q_1 + \Delta z} + \frac{\sin^2\theta}{q_2 + \Delta z} & \frac{1}{2}\sin 2\theta\left(\frac{1}{q_1 + \Delta z} - \frac{1}{q_2 + \Delta z}\right) \\ \frac{1}{2}\sin 2\theta\left(\frac{1}{q_1 + \Delta z} - \frac{1}{q_2 + \Delta z}\right) & \frac{\sin^2\theta}{q_1 + \Delta z} + \frac{\cos^2\theta}{q_2 + \Delta z} \end{pmatrix}. \qquad (10)$$

Therefore, the propagation law for a general astigmatic Gaussian beam is identical to the one for a simple astigmatic Gaussian beam:

$$q'_j = q_j + \Delta z, \qquad j = 1, 2. \qquad (11)$$

The complex angle θ remains unaffected along the propagation.

The amplitude $E_0(z)$ can be computed from the fact that the overall beam power at every cross section is equal to the integral of the intensity of the beam. This power does not depend on z if we integrate over the entire XY plane,

$$P = \iint_{XY} I(x,y,z)\mathrm{d}x\mathrm{d}y. \qquad (12)$$

The intensity of the beam can be represented as

$$\begin{aligned}
I(x,y,z) &= |E(x,y,z)|^2 \\
&= E_0(z)^2\exp(g_1(z)x^2 + g_2(z)y^2 + g(z)xy), \quad (13)
\end{aligned}$$

where

$$\begin{aligned}
g_1(z) &= k\Im(Q_{11}), \\
g_2(z) &= k\Im(Q_{22}), \\
g(z) &= k\Im(Q_{12} + Q_{21}), \qquad (14)
\end{aligned}$$

and Q_{ij} stands for the ij element of the complex radius of curvature tensor $Q(z)$. Substituting Eq. (13) into Eq. (12), and computing the double integral using the Euler–Poisson (Gaussian) integral, we obtain

$$P = E_0^2(z) \frac{2\pi}{\sqrt{4g_1(z)g_2(z) - g^2(z)}}, \qquad (15)$$

$$E_0(z) = \sqrt{\frac{P}{\lambda}\sqrt{4\Im(Q_{11})\Im(Q_{22}) - \Im(Q_{12} + Q_{21})^2}}. \quad (16)$$

From Eqs. (5), (6), (9), and (11) it follows that in order to fully describe a general astigmatic Gaussian beam one can choose either of two strategies. The first one is the use of three complex-valued parameters: two q-parameters $q_j, j = 1, 2$, and one complex angle θ. The other possible strategy is to use the complex radius of curvature tensor [Eq. (7)]. Both strategies are connected: the reciprocals of q_1 and q_2 are the eigenvalues of the complex radius of curvature tensor, and θ can be obtained from Q using the relationship

$$\tan 2\theta = \frac{Q_{12} + Q_{21}}{Q_{11} - Q_{22}}. \qquad (17)$$

3. Intensity and Phase Distributions

All values discussed in the previous section are complex-valued and therefore do not have a direct physical meaning. For the Gaussian beams with simple astigmatism each q-parameter can be interpreted as shown in Eq. (2). Another valid interpretation is

$$q_j = z - z_{0j} + iz_{Rj}, \qquad j = 1, 2, \qquad (18)$$

where z_{0j} is the waist position and z_{Rj} is the Rayleigh range of the beam in one of its principal planes. The real-valued angle θ for a simple astigmatic Gaussian beam shows the rotation of the beam's principal coordinate system with respect to the global coordinate system.

For the general astigmatic Gaussian beam, none of these interpretations hold. In order to obtain real-valued parameters, we can separate the real and imaginary parts of the complex phase in Eq. (6):

$$E(\mathbf{r}, z) = E_0(z) \exp\left\{\frac{k}{2}\mathbf{r}^T\Im(Q)\mathbf{r}\right\}$$
$$\times \exp\left\{-i\frac{k}{2}\mathbf{r}^T\Re(Q)\mathbf{r} - i\phi_{\mathrm{ac}} + i\eta(z)\right\}. \quad (19)$$

Let us now define the matrices,

$$W(z) = -(k/2)\Im(Q), \qquad C(z) = \Re(Q). \qquad (20)$$

For the simple astigmatic Gaussian beams in their principal coordinate system, they represent the ellipses of constant intensity and constant phase, respectively,

$$W_{\mathrm{SA}}(z) = \begin{pmatrix} \frac{1}{w_x^2(z)} & 0 \\ 0 & \frac{1}{w_y^2(z)} \end{pmatrix}, \qquad C_{\mathrm{SA}}(z) = \begin{pmatrix} \frac{1}{R_x(z)} & 0 \\ 0 & \frac{1}{R_y(z)} \end{pmatrix}, \quad (21)$$

Substituting Eq. (20) into Eq. (19), we obtain (see [11])

$$E(\mathbf{r}, z) = E_0(z) \exp\{-\mathbf{r}^T W(z)\mathbf{r}\}$$
$$\times \exp\left\{-i\frac{k}{2}\mathbf{r}^T C(z)\mathbf{r} - i\phi_{\mathrm{ac}} + i\eta(z)\right\}. \quad (22)$$

For the general astigmatic beam, the matrices defined in Eq. (20) still represent the ellipses of constant intensity and of constant phase. In the same way as the complex radius of curvature tensor for generalized Gaussian beams [Eq. (7)], they become

$$W_{\mathrm{GA}}(z)$$
$$= \begin{pmatrix} \frac{\cos^2\varphi_w}{w_1^2(z)} + \frac{\sin^2\varphi_w}{w_2^2(z)} & \frac{1}{2}\sin 2\varphi_w\left(\frac{1}{w_1^2(z)} - \frac{1}{w_2^2(z)}\right) \\ \frac{1}{2}\sin 2\varphi_w\left(\frac{1}{w_1^2(z)} - \frac{1}{w_2^2(z)}\right) & \frac{\sin^2\varphi_w}{w_1^2(z)} + \frac{\cos^2\varphi_w}{w_2^2(z)} \end{pmatrix},$$
$$C_{\mathrm{GA}}(z)$$
$$= \begin{pmatrix} \frac{\cos^2\varphi_R}{R_1(z)} + \frac{\sin^2\varphi_R}{R_2(z)} & \frac{1}{2}\sin 2\varphi_R\left(\frac{1}{R_1(z)} - \frac{1}{R_2(z)}\right) \\ \frac{1}{2}\sin 2\varphi_R\left(\frac{1}{R_1(z)} - \frac{1}{R_2(z)}\right) & \frac{\sin^2\varphi_R}{R_1(z)} + \frac{\cos^2\varphi_R}{R_2(z)} \end{pmatrix}. \quad (23)$$

Note that, for simple astigmatic beams tilted by a real-valued angle θ around the z axis, Eq. (23) holds with $\varphi_w = \varphi_R = \theta$. The eigenvalues $1/w_j^2, j = 1, 2$ of the matrix $W(z)$ are reciprocals of the principal axes of the intensity ellipse squared. Similarly, the eigenvalues $1/R_j, j = 1, 2$ of the matrix $C(z)$ are the reciprocals of the principal radii of curvature of the wavefront. The orientation of ellipses is described by the angles φ_w and φ_R, which can be obtained in the same way as angle θ in Eq. (17),

$$\tan 2\varphi_w = \frac{W_{12} + W_{21}}{W_{11} - W_{22}}, \qquad (24)$$

$$\tan 2\varphi_R = \frac{C_{12} + C_{21}}{C_{11} - C_{22}}. \qquad (25)$$

Equations (24), (25) and the eigenvalue computation are already sufficient for the computation of the intensity and phase distribution of any Gaussian beam in the fundamental mode. However, they do not provide a direct description of general astigmatic Gaussian beam characteristics. In order to study these more closely, we can substitute

$$\theta = \alpha + i\beta,$$

$$1/q_j = \rho_j - i\omega_j, \qquad j = 1, 2,$$

$$\rho_j(z) = \Re(q_j)/|q_j|^2,$$

$$\omega_j(z) = \Im(q_j)/|q_j|^2, \tag{26}$$

in the complex radius of curvature tensor $Q(z)$ [Eq. (7)] and obtain the matrices $W(z)$ and $C(z)$ from Eq. (20). Then, using Eqs. (24), (25), the values for the angles φ_w and φ_R of the intensity and phase ellipses are

$$\tan 2\varphi_{w0}(z) = -\frac{\rho_1(z) - \rho_2(z)}{\omega_1(z) - \omega_2(z)} \tanh 2\beta,$$

$$\varphi_w(z) = \varphi_{w0}(z) + \alpha, \tag{27}$$

$$\tan 2\varphi_{R0}(z) = \frac{\omega_1(z) - \omega_2(z)}{\rho_1(z) - \rho_2(z)} \tanh 2\beta,$$

$$\varphi_R(z) = \varphi_{R0}(z) + \alpha. \tag{28}$$

The eigenvalues of the matrices $W(z)$ and $C(z)$ can be expressed as

$$\frac{1}{w_{1,2}^2(z)}$$

$$= \frac{k}{4}\Big\{ \omega_1(z) + \omega_2(z)$$

$$\pm \sqrt{[\omega_1(z) - \omega_2(z)]^2 \cosh^2 2\beta + [\rho_1(z) - \rho_2(z)]^2 \sinh^2 2\beta} \Big\}, \tag{29}$$

$$\frac{1}{R_{1,2}(z)}$$

$$= \frac{1}{2}\Big\{ \rho_1(z) + \rho_2(z)$$

$$\pm \sqrt{[\rho_1(z) - \rho_2(z)]^2 \cosh^2 2\beta + [\omega_1(z) - \omega_2(z)]^2 \sinh^2 2\beta} \Big\}. \tag{30}$$

Equations (27)–(30) introduce the physical meaning of the complex parameters of general astigmatic Gaussian beams. They allow the ellipses of constant intensity and the ellipses of constant phase in the medium to be obtained. In the simple astigmatic case, each principal axis of the beam spot ellipse and the phase ellipse can be computed from a single q-parameter using Eq. (2). However, in the general astigmatic case, each real-valued parameter is computed using both q-parameters and the value of the complex angle θ. Therefore, a single q-parameter or angle θ alone does not have a direct physical interpretation for general astigmatic beams.

The complex angle θ (and thus both α and β) does not change along the propagation [Eq. (11)]. Its real part α is one of the two terms for both angles φ_w and φ_R [Eqs. (27) and (28)] and it does not couple into the principal axes of the ellipses of constant intensity and constant phase [Eqs. (29) and (30)]. These two facts allow the interpretation of α as the angle of rotation of the entire beam. It is always possible to choose a beam-fixed coordinate system where α is zero. The imaginary part β causes the orientations of both ellipses of constant intensity and of constant phase (φ_w and φ_R) to change along the propagation [Eqs. (27) and (28)]. In order to study this dependence, we will illustrate the evolution of the two q parameters [Eq. (26)] by a Gaussian beam [or Collins [9]] chart (Fig. 2). The evolution of each of the two q-parameters is represented by a circle with a diameter of $1/\Im(q)$. The line connecting two circles at identical values of z changes the angle with the ω axis monotonically by a total of 2π as z goes from $-\infty$ to $+\infty$. The tangent of this angle for each value of z is $(\rho_1 - \rho_2)/(\omega_1 - \omega_2)$. This value is used in both Eqs. (27) and (28). Therefore, both φ_w and φ_R change monotonically with increasing z. Depending on the value of β, angles can either increase or decrease. Each angle changes by a total of π radians from $z = -\infty$ to $z = \infty$. Experimental observation over the infinite range is impossible, but by choosing to observe the regions with maximum slope $\partial\varphi_w/\partial z$ (or $\partial\varphi_R/\partial z$) one can see most of the overall rotation of the ellipse of constant intensity (or ellipse of constant phase).

The relative orientation of the ellipses of constant intensity and constant phase [from Eqs. (27) and (28)] is described by
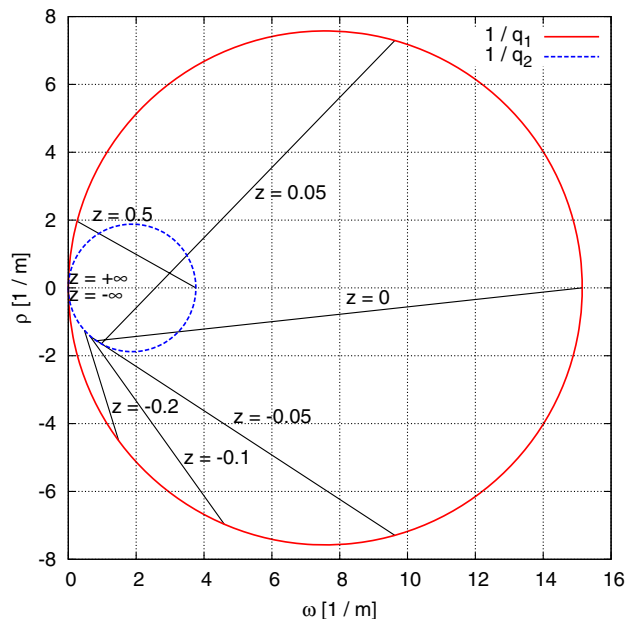

Fig. 2. Gaussian beam (or Collins) chart. $q_1 = i66$ mm, $q_2 = -500 + i266$ mm at $z = 0$. The axes are $\omega(z) = \Im(q)/|q|^2$ and $\rho(z) = \Re(q)/|q|^2$. The line connecting two circles for the same value of z forms an angle, with tangent $(\rho_1 - \rho_2)/(\omega_1 - \omega_2)$, with the ω axis.

$$\tan 2(\varphi_w(z) - \varphi_R(z))$$

$$= -\sinh 2\beta \cosh 2\beta \left(\frac{\rho_1(z) - \rho_2(z)}{\omega_1(z) - \omega_2(z)} + \frac{\omega_1(z) - \omega_2(z)}{\rho_1(z) - \rho_2(z)} \right). \tag{31}$$

This equation shows that the ellipses can only be aligned (have a relative angle of 0 or $\pi/2$) at a given point z' if either $\beta = 0$ or $q_1(z') = q_2(z')$. According to the law of propagation [Eq. (11)], this is only possible for special cases of simple astigmatism or perfect stigmatism. Thus, the ellipses of constant intensity and constant phase cannot be aligned at any point along the propagation for general astigmatic beams. Similarly, it can be shown that spot ellipses and wavefronts of the general astigmatic Gaussian beam never degenerate to circles. Equation (31) shows that the relative orientation changes along the z axis. Only the invariant

$$\tan 2\varphi_{w0}(z) \tan 2\varphi_{R0}(z) = -\tanh^2 2\beta \tag{32}$$

is independent of z.

The evolution of the beam width is presented in Fig. 3 for simple and general astigmatic Gaussian beams with identical q-parameters. The corresponding graphs for the major and minor semi-axes of both ellipses of constant phase and constant intensity are shown in Fig. 4. For simple astigmatic beams, waist positions and Rayleigh ranges can be found from the q-parameters using Eq. (18) separately in each of the planes of symmetry. The minimal wavefront radius of curvature, in this case, is achieved where $z = z_{0j} \pm z_{Rj}$ and is equal to $2z_{Rj}$. This physical interpretation no longer holds for general astigmatic Gaussian beams. Let us estimate the expression under the square root sign in Eq. (29):

$$[\omega_1(z) - \omega_2(z)]^2 \underbrace{\cosh^2 2\beta}_{\geq 1} + \underbrace{[\rho_1(z) - \rho_2(z)]^2 \sinh^2 2\beta}_{\geq 0}$$

$$\geq [\omega_1(z) - \omega_2(z)]^2, \tag{33}$$

and equality holds only in the simple astigmatic case. This means that, for any value of β,

$$\frac{1}{w_{2\mathrm{GA}}^2(z)} < \frac{1}{w_{1,2\mathrm{SA}}^2(z)} < \frac{1}{w_{1\mathrm{GA}}^2(z)}, \tag{34}$$

where $w_{1,2\mathrm{GA}}(z)$ are the major and minor semi-axes of the intensity ellipse of the general astigmatic beam, $w_{1,2\mathrm{SA}}(z)$ are the semi-axes of the intensity ellipse of the simple astigmatic beam with identical q-parameters. Taking into account that all values of spot radii are positive, this is equivalent to

$$w_{1\mathrm{GA}}(z) < w_{1,2\mathrm{SA}}(z) < w_{2\mathrm{GA}}(z), \tag{35}$$

for any value of z. This fact is illustrated in Fig. 4(a) and effectively means that, for any general

(a)

(b)
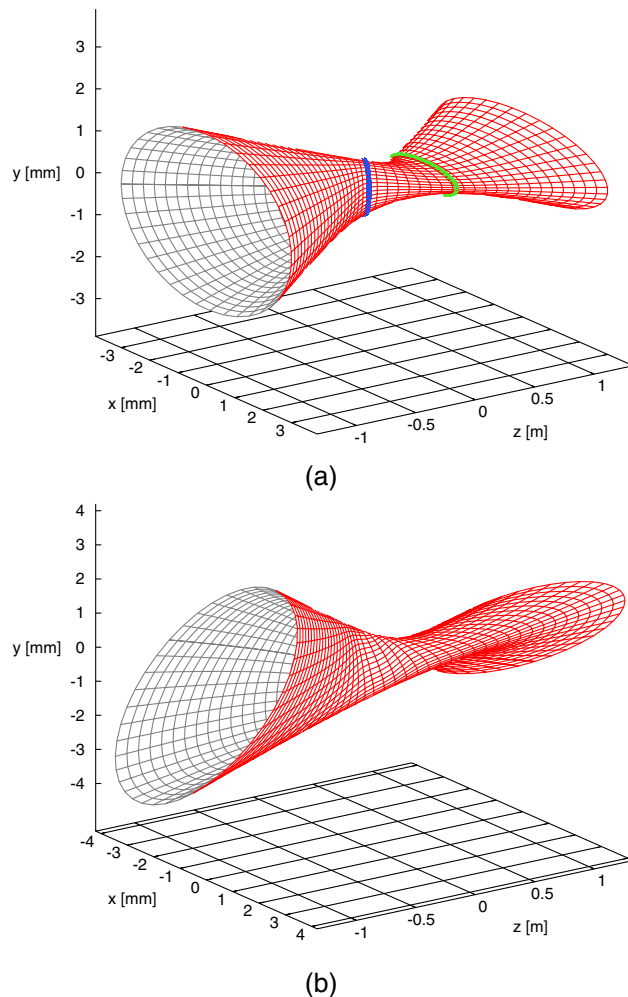
Fig. 3. Beam width evolution of (a) simple and (b) general astigmatic Gaussian beams with identical q-parameters and optical wavelengths ($\lambda = 1064$ nm; $q_1 = i66$ mm, $q_2 = -500 + i266$ mm at $z = 0$; $q_1 = 500 + i66$ mm, $q_2 = i266$ mm at $z = 0.5$ m). The complex angle for the general astigmatic beam is $\theta = 20° + i10°$. In the simple astigmatic case one can observe two waists in two orthogonal planes (blue ring (left) corresponds to the waist in the XZ plane reached at $z = 0$, green ring (right) corresponds to the waist in YZ plane reached at $z = 0.5$ m). In the general astigmatic case waists cannot be defined.

astigmatic Gaussian beam, its ellipses of constant intensity have higher ellipticity than for the corresponding simple astigmatic Gaussian beam. Similarly,

$$\frac{1}{R_{2\mathrm{GA}}(z)} < \frac{1}{R_{1,2\mathrm{SA}}(z)} < \frac{1}{R_{1\mathrm{GA}}(z)}, \tag{36}$$

where $R_{1,2\mathrm{GA}}(z)$ are the principal radii of curvature of the wavefronts of the general astigmatic Gaussian beam, and $R_{1,2\mathrm{SA}}(z)$ are the principal radii of curvature of the wavefronts of the corresponding simple astigmatic Gaussian beam. Since some of those radii can be negative, we cannot draw the same conclusion as for spot radii [see Fig. 4(b)].

Fig. 4. (a) Beam width evolution and (b) radius of curvature of the wavefront evolution for a general astigmatic Gaussian beam in comparison to the same quantities for a simple astigmatic Gaussian beam with identical q-parameters and optical wavelength. $q_1 = i66$ mm, $q_2 = -500 + i266$ mm at $z = 0$. $\lambda = 1064$ nm. The complex angle for the general astigmatic beam is $\theta = 20° + i10°$. For any value of z: $w_{1GA}(z) < w_{1,2SA}(z) < w_{2GA}(z)$, $w_{1GA}(z) \neq w_{2GA}(z)$.

The value of β cannot be arbitrary. The semi-axes of the spot ellipse should always be positive [4]:

$$\omega_1 + \omega_2 \geq \sqrt{(\omega_1 - \omega_2)^2 \cosh^2 2\beta + (\rho_1 - \rho_2)^2 \sinh^2 2\beta}, \tag{37}$$

$$\cosh^2 2\beta \leq \left| \frac{q_1 - q_2^*}{q_1 - q_2} \right|. \tag{38}$$

This condition is independent of z.

We have shown that the parameters of intensity and phase distributions of the general astigmatic Gaussian beam can be obtained from the radius of curvature tensor $Q(z)$, using eigenvalue computation and the simple Eqs. (24) and (25). Alternatively, one

can use Eqs. (27)–(30) to compute these parameters from complex-valued q-parameters and the angle θ.

4. Beam Transformation

In order to obtain the formulas for general astigmatic Gaussian beam transformation via reflection or refraction, we will generally follow the procedure proposed in [5]. In our derivations we will add the possibility of choosing beam-fixed and surface-fixed transversal coordinate vectors, arbitrarily. We will use the fact that the complex phase [Eq. (8)] of incident, reflected, and refracted beams should match exactly on the surface. This is, therefore, an extension of the phase matching method described in [12,13]. We will assume that, at the point of incidence, the beam radii are small in comparison to the radii of curvature of the surface.

Any second-order 3D surface (sphere, ellipsoid, cylinder etc.) can be described by a quadratic equation,

$$\hat{s}(\mathbf{d}) = d_1 \hat{d}_1 + d_2 \hat{d}_2 - \frac{1}{2} (\mathbf{d}^T C_s \mathbf{d}) \hat{n}, \tag{39}$$

where $\mathbf{d}$ is a 2D vector with components d_1 and d_2, $(\hat{d}_1, \hat{d}_2, \hat{n})$ in a local coordinate system describing a surface at the point of incidence (see Fig. 5) such that $\hat{n}$ is a vector normal to the surface and $\hat{d}_1$ and $\hat{d}_2$ are unit vectors in the plane tangential to the surface. $\hat{d}_1$ and $\hat{d}_2$ can be chosen arbitrarily, but the coordinate system has to stay orthonormal. C_s is the curvature matrix of the surface in the local coordinate system. Any higher-order surface can be approximated using Eq. (39).

If the surface equation in the local coordinate system is given, one can obtain its curvature matrix C_s as the second-order derivative at the point of incidence. For example, the ellipsoid with the principal semi-axes A, B, and C (see Fig. 5) in its nominal

Fig. 5. Geometry of the reflection and transmission of a general astigmatic Gaussian beam.

coordinate system, placed in the center of the ellipsoid, is represented by

$$f(\mathbf{x}) = \mathbf{x}^T S \mathbf{x} - 1 = 0, \qquad (40)$$

where

$$S = \begin{pmatrix} 1/A^2 & 0 & 0 \\ 0 & 1/B^2 & 0 \\ 0 & 0 & 1/C^2 \end{pmatrix}, \qquad (41)$$

and $\mathbf{x} = (x, y, z)$ is a coordinate vector. If we rewrite this equation in the local coordinate system using the affine transformation $\mathbf{x}' = M\mathbf{x} + \mathbf{t}$, where $\mathbf{t}$ is a vector connecting the center of the ellipsoid with the point of incidence, and M is a rotation matrix from the nominal ellipsoid coordinate system into the local coordinate system, we obtain

$$f(\mathbf{x}') = (\mathbf{x}' - \mathbf{t})^T S' (\mathbf{x}' - \mathbf{t}) - 1 = 0. \qquad (42)$$

Here, $S' = MSM^T$. From this equation, we need to derive z' as a function of (x', y') and find the curvature matrix as its second-order derivative,

$$C_s = \begin{pmatrix} \partial^2 z'/\partial x'^2 & \partial^2 z'/\partial x' \partial y' \\ \partial^2 z'/\partial y' \partial x' & \partial^2 z'/\partial y'^2 \end{pmatrix}. \qquad (43)$$

Skipping lengthy calculations, the curvature matrix of an ellipsoid at a point on its surface is equal to

$$
\begin{aligned}
&C_{\text{ellipsoid}} \\
&= \pm \frac{1}{b} \begin{pmatrix} S'_{11} S'_{33} - S'^2_{13} + g t_y^2 & S'_{12} S'_{33} - S'_{13} S'_{23} - g t_x t_y \\ S'_{12} S'_{33} - S'_{13} S'_{23} - g t_x t_y & S'_{22} S'_{33} - S'^2_{23} + g t_x^2 \end{pmatrix},
\end{aligned}
$$
$$\qquad (44)$$

where

$$
\begin{aligned}
b &= [(S'_{13} t_x + S'_{23} t_y)^2 - S'_{33}(S'_{11} t_x^2 + 2 S'_{12} t_x t_y + S'_{22} t_y^2 - 1)]^{3/2}, \\
g &= S'_{11} S'^2_{23} + S'_{22} S'^2_{13} + S'_{33} S'^2_{12} - 2 S'_{12} S'_{13} S'_{23} - S'_{11} S'_{22} S'_{33},
\end{aligned}
$$
$$\qquad (45)$$

and S'_{ij} are the elements of matrix S'. Equation (44) can also be used for cylindrical surfaces ($1/A^2$ or $1/B^2$ should then be set to 0). In the special case of spherical surfaces, the curvature matrix is the same at every point of the surface:

$$C_{\text{sphere}} = \pm \begin{pmatrix} c & 0 \\ 0 & c \end{pmatrix}, \qquad (46)$$

where $1/c$ is the radius of the sphere.

Now, let us introduce three beam-fixed coordinate systems $(\hat{x}_l, \hat{y}_l, \hat{z}_l)$ for $l = i, r, t$ for incident, reflected, and transmitted beams, respectively (Fig. 5). Similar to the ray-fixed coordinate system from [13], $\hat{z}_l$ corresponds to the direction of beam propagation and the

transversal unit vectors, $\hat{x}_l$ and $\hat{y}_l$, can be chosen arbitrarily such that coordinate system $(\hat{x}_l, \hat{y}_l, \hat{z}_l)$ stays orthonormal. The directions of the beams are connected via the law of reflection,

$$\hat{z}_r = \hat{z}_i - 2(\hat{z}_r \cdot \hat{n})\hat{n}, \qquad (47)$$

and the law of refraction (Snell's law) [14],

$$\hat{z}_t = \frac{n_i}{n_t}\hat{z}_i + \left(\cos\theta_t - \frac{n_i}{n_t}\cos\theta_i \right)\hat{n}, \quad n_i \sin\theta_i = n_t \sin\theta_t, \qquad (48)$$

where n_i and n_t are the refractive indices of the two media, $\cos\theta_i = -\hat{n}\hat{z}_i$, and $\cos\theta_t = -\hat{n}\hat{z}_t$.

For each of the three beams, the complex radius of curvature tensor $Q_l(z_l)$ is given in a corresponding coordinate system $(\hat{x}_l, \hat{y}_l, \hat{z}_l)$. The complex phase [Eq. (8)] of each of the three beams in their beam-fixed coordinate system is

$$\phi(\mathbf{r}_l, z_l) = -k_l \left(z_l + \frac{1}{2}\mathbf{r}_l^T Q_l(z_l)\mathbf{r}_l \right), \qquad l = i, r, t, \quad (49)$$

where $\mathbf{r}_l$ is a vector of transversal coordinates x_l and y_l in a beam-fixed coordinate system $(\hat{x}_l, \hat{y}_l, \hat{z}_l)$. We neglect the slowly varying Gouy phase $\eta(z)$ [9], since it can be computed independently using Eq. (4). In order to keep the Gouy phase continuous, the accumulated Gouy phase can be used as described in [7]. The term ϕ_{ac} can be represented as $\phi_{\text{ac}} = \bar{\phi}_{\text{ac}} + k_l z_l$, where phase $\bar{\phi}_{\text{ac}}$ is accumulated before the beam transformation and is thus identical for the incident, reflected, and refracted beam. Therefore, we can replace ϕ_{ac} with $k_l z_l$ in the phase matching.

The points (x_l, y_l, z_l) on a surface [Eq. (39)] can be found from

$$
\begin{aligned}
x_l &= \hat{s}(\mathbf{d})\hat{x}_l = d_1 \hat{x}_l \hat{d}_1 + d_2 \hat{x}_l \hat{d}_2 - 1/2(\mathbf{d}C_s \mathbf{d}^T)\hat{x}_l \hat{n}, \\
y_l &= \hat{s}(\mathbf{d})\hat{y}_l = d_1 \hat{y}_l \hat{d}_1 + d_2 \hat{y}_l \hat{d}_2 - 1/2(\mathbf{d}C_s \mathbf{d}^T)\hat{y}_l \hat{n}, \\
z_l &= \hat{s}(\mathbf{d})\hat{z}_l = d_1 \hat{z}_l \hat{d}_1 + d_2 \hat{z}_l \hat{d}_2 - 1/2(\mathbf{d}C_s \mathbf{d}^T)\hat{z}_l \hat{n}. \quad (50)
\end{aligned}
$$

If we introduce

$$K_l = \begin{pmatrix} \hat{x}_l \hat{d}_1 & \hat{x}_l \hat{d}_2 \\ \hat{y}_l \hat{d}_1 & \hat{y}_l \hat{d}_2 \end{pmatrix}, \qquad l = i, r, t, \qquad (51)$$

Equation (50) can be split into two terms:

$$\mathbf{r}_l = K_l \mathbf{d} - \frac{1}{2}(\mathbf{d}C_s \mathbf{d}^T) \cdot \begin{pmatrix} \hat{x}_l \hat{n} \\ \hat{y}_l \hat{n} \end{pmatrix},$$

$$z_l = d_1 \hat{z}_l \hat{d}_1 + d_2 \hat{z}_l \hat{d}_2 - \frac{1}{2}(\mathbf{d}C_s \mathbf{d}^T)\hat{n}\hat{z}_l. \qquad (52)$$

Ignoring the second-order term for the transversal coordinates [12] and substituting the result into Eq. (49), we obtain

$$\phi_l = -k_l \Big((\hat{z}_l \hat{d}_1) d_1 + (\hat{z}_l \hat{d}_2) d_2 - \frac{1}{2} (\mathbf{d} C_s \mathbf{d}^T) \hat{n} \hat{z}_l$$

$$+ \frac{1}{2} (K_l \mathbf{d})^T Q_l(z_l) (K_l \mathbf{d}) \Big)$$

$$= -k_l \underbrace{((\hat{z}_l \hat{d}_1) \hat{d}_1 + (\hat{z}_l \hat{d}_2) \hat{d}_2)}_{p_l} (d_1 \hat{d}_1 + d_2 \hat{d}_2)$$

$$- \frac{1}{2} k_l \mathbf{d}^T \underbrace{(K_l^T Q_l(z_l) K_l - C \hat{n} \hat{z}_l)}_{\Gamma_l} \mathbf{d}. \tag{53}$$

Here, p_l is a projection of the beam direction $\hat{z}_l$ on a plane that is tangential to the surface at the point of incidence. Since the beam radii are much smaller than the radii of curvature of the surface, we can assume that Q_l is constant on a surface and is equal to its value at the point of incidence.

Linear and quadratic terms of the complex phases should be matched separately. The linear term confirms Snell's law and the quadratic term allows the equations for the complex radius of curvature tensor of reflected and transmitted beams to be obtained,

$$k_i \Gamma_i = k_i \Gamma_r = k_t \Gamma_t, \tag{54}$$

which yields

$$Q_r = (K_r^T)^{-1} (K_i^T Q_i K_i - C(\hat{n} \hat{z}_i - \hat{n} \hat{z}_r)) K_r^{-1}, \tag{55}$$

$$Q_t = \frac{n_1}{n_2} (K_t^T)^{-1} \Big(K_i^T Q_i K_i - C\Big(\hat{n} \hat{z}_i - \frac{n_2}{n_1} \hat{n} \hat{z}_t \Big) \Big) K_t^{-1}. \tag{56}$$

Therefore, we derived the equations for the complex radius of curvature tensor of reflected and refracted beams, for the case of an arbitrary 3D surface, approximated by a quadratic equation. Lenses and other multisurface structures can be analyzed by considering multiple reflections and refractions from each of the surfaces that make up such structures.

Eqs. (55) and (56) do not only correct the typos in [5], but also allow different possible notations for beam-fixed and surface-fixed coordinate systems. Only the beam directions $\hat{z}_l$ and surface normal ($\hat{n}$) at the point of incidence should stay fixed, while transversal coordinate vectors ($\hat{x}_l, \hat{y}_l, \hat{d}_1, \hat{d}_2$) can be chosen arbitrarily in the plane that is tangential to the surface at the point of incidence. We also believe that using the given vector notation is more reliable than substituting angles of incidence, reflection, and refraction, since it does not require sign checks.

5. Experimental Verification of the Model

In order to verify the model experimentally, we transmitted a well-characterized Gaussian laser beam through two cylindrical lenses and characterized the beam intensity distribution behind the second lens. The lenses were set up in such a way that an elliptical beam with a rotating ellipse was formed

from the nearly round initial beam. Using Eq. (56), from the measured parameters of the initial beam and the lenses we computed the beam intensity distributions at different positions along the optical axis behind the second lens and compared it to the measured beam intensity distributions. In order to minimize the effect of measurement uncertainties of the individual parameters, we then fitted these parameters to the measured beam intensity distributions.

In Fig. 6 the schematic of the experimental setup is shown. The light from a laser (Mephisto 500 by Coherent), with a wavelength of $\lambda = 1064$ nm, was coupled into a single-mode polarisation-maintaining fiber with angle-polished connectors that acted as a spatial mode filter. The light emitted by the fiber was collimated with an aspherical lens with 11 mm focal length (60FC-4-A11-03 by Schäfter und Kirchhoff). The principal beam radii w_1 and w_2 were measured at several distances z_j from the fiber collimator using the WinCamD-UCD23 by Dataray. The waist radii w_{01} and w_{02} and distances between the fiber collimator and waists z_{01} and z_{02} were obtained using a least squares fit of the beam radii evolution of the simple astigmatic Gaussian beam,

$$w_i(z) = w_{0i} \sqrt{1 + \left(\lambda \frac{z - z_{0i}}{\pi w_{0i}^2} \right)^2}, \qquad i = 1, 2, \tag{57}$$

to the measured beam radii $w_i(z_j)$, $i = 1, 2$. The CCD camera also measured the transversal tilt φ_{w0} of the beam with respect to the laboratory coordinate system.

After the initial simple astigmatic beam was fully characterized, we transformed it into a general astigmatic beam using two cylindrical lenses tilted with respect to each other in the transversal plane xy. The lenses were placed at distances z_1 and z_2 from the fiber collimator and tilted by angles α_1 and α_2 around the optical axis ($\alpha_j = 0$ stands for no curvature in the horizontal direction). Their focal lengths were f_1 and f_2, respectively.
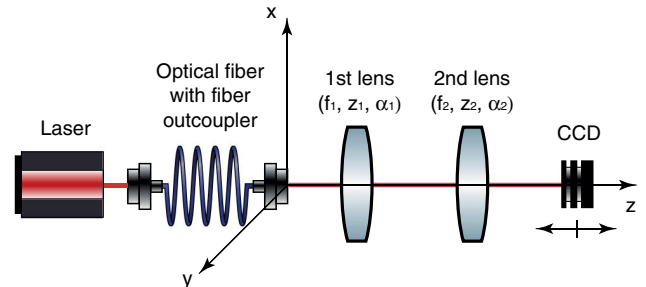

Fig. 6. Simplified schematic of the experiment. The output from a laser was coupled into a fiber acting as a special mode filter. First, the beam exiting the fiber was characterized using the CCD camera, then two cylindrical lenses (focal length f_i, distance to fiber collimator z_i, angle α_i to y axis) were inserted and the resulting beam intensity pattern was measured with the CCD camera at different positions behind the second lens.

Table 1. Parameters of the Setup, Including Measured Values, Tolerances, and Fitted Values

Parameter	Units	Value	Tolerance	Fit
λ	[nm]	1064	0	1064
w_{01}	[μm]	218	±12.2	207
w_{02}	[μm]	213	±14	227
z_{01}	[mm]	0.7	±5	−2.5
z_{02}	[mm]	0.2	±5.7	5.9
φ_{w0}	[deg]	0	±90	1.5
f_1	[mm]	53.5	±3.7	49.9
f_2	[mm]	66.5	±4.6	68.2
z_1	[mm]	10	0	10
α_1	[deg]	0	0	0
z_2	[mm]	208	±1	209
α_2	[deg]	17	±1	16.6
l_{CCD}	[mm]	7.2	±1	6.2
β_{CCD}	[deg]	0	±1	−0.6

The chip depth from the front of the case of the CCD camera l_{CCD} should be taken into account. The camera was aligned to the global coordinate system, but its small residual tilt around the z axis was accounted for by the angle β_{CCD}. The camera could be used to measure beam radii of up to 1.25 mm.

After the general astigmatic beam was produced, its intensity profile was characterized using the same CCD camera at different distances behind the second lens. From this characterization we obtained the principal beam radii w_1 and w_2 and the angles of the beam ellipse φ_w at different positions along the optical axis z. We did not only perform the direct comparison of these measured values with the corresponding simulated results. Instead, we assumed that each parameter of our optical system is measured with some tolerance. In order to conclude that experimental and simulated results matched, we fitted simulation results to the measured data by varying the measured parameters within their tolerances. Not every parameter needed to be varied. Changing the positions of both waists produces the same effect as changing the position of the first lens. Similarly, the initial beam tilt and the first lens tilt cannot be distinguished. Therefore, we assumed no tolerance for the first lens position z_1 and angle α_1. The value of the optical wavelength λ was also assumed to be precise. The linear measurements performed with the ruler assumed a possible error of either 1 mm (z_2, l_{CCD}), or 1 deg (α_2, β_{CCD}). The focal lengths were measured twice, with a possible error of up to 10% per measurement. Therefore, their overall tolerance was $10\%/\sqrt{2} \approx 7\%$. For the initial beam parameters, the confidence intervals given by the fit to the simple astigmatic model were taken as the tolerance values. We assumed that the beam angle can have any possible value since the beam is nearly circular ($w_{01}/w_{02} \approx 1.02$). All parameters including their measured values, tolerances, and fitted values are summarized in Table 1.

In Figs. 7, 8 the comparison of the measured and simulated beam intensity ellipses is illustrated. Fig. 7(a) shows the angle of the intensity ellipse with
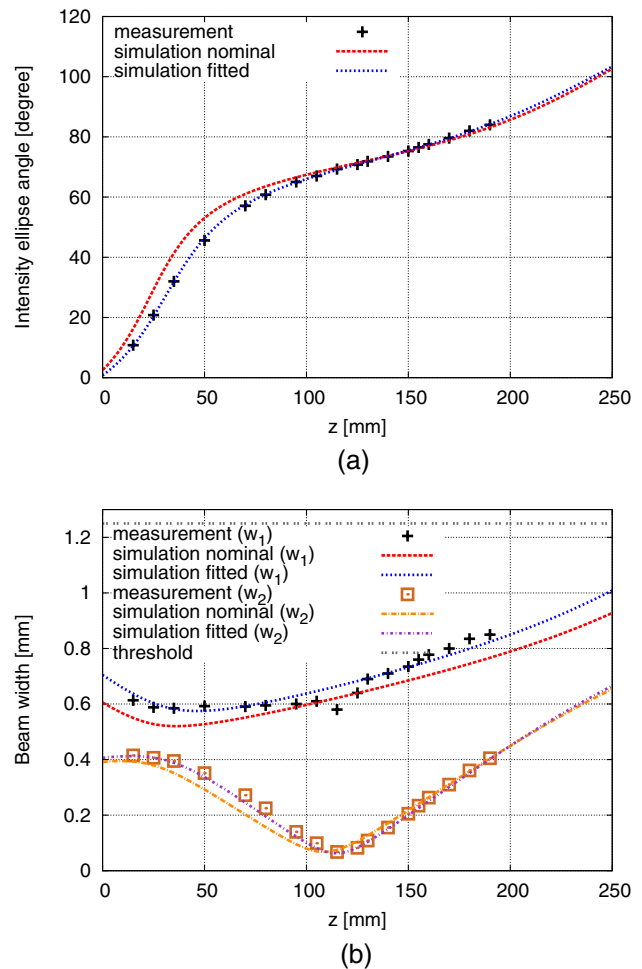

Fig. 7. (a) Intensity ellipse angle, and (b) semi-axes along the propagation behind the second lens. Measured points and simulated curves with nominal and fitted parameters (see Table 1). The threshold on the graph (b) is the maximum beam radius that can be measured by the CCD-camera.

respect to the horizontal axis over the distance from the second lens. Fig. 7(b) illustrates the evolution of the major and minor semi-axes of the beam ellipse over the distance from the second lens. The measured values are shown as black plus signs and brown square signs, the simulation with independently measured parameters is shown as red dashed and orange long dashed–dotted lines, and the simulation with fitted parameters is shown as blue dotted and magenta dashed–dotted lines. In Fig. 8 one can see the intensity distributions of the general astigmatic Gaussian beam at a different distances behind the second lens, both produced by the CCD camera and simulated with the model using the fitted parameter values. The simulation with nominal parameters already agrees well with the measured data. After fitting the parameters, simulation and measurement have even better agreement, proving that the suggested model is capable of precisely describing the experiment and can be used in theoretical investigations of the behavior of Gaussian beams in the fundamental mode in different optical systems.
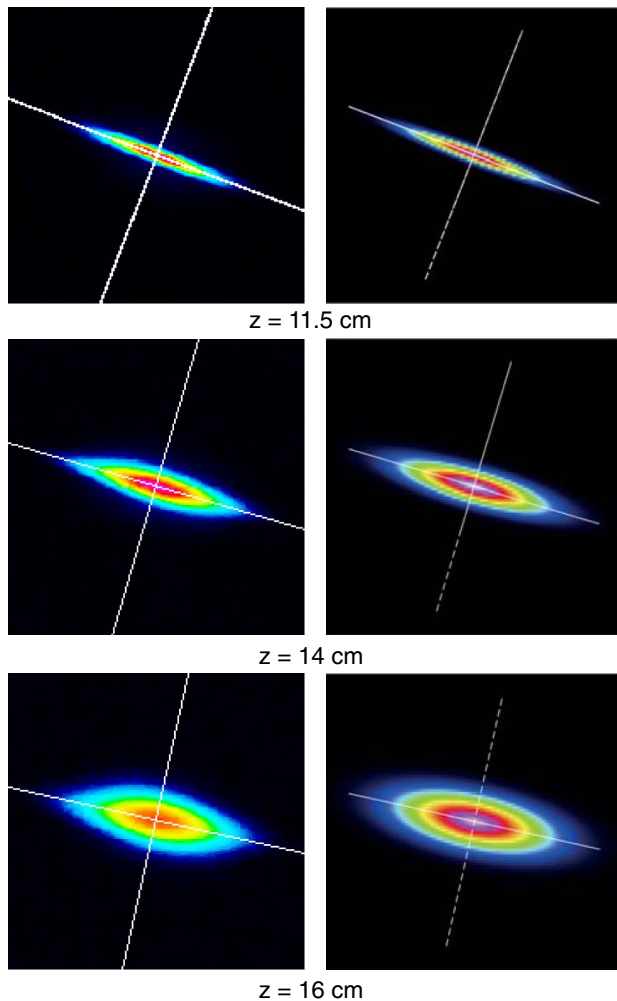
Fig. 8. Measured (left column) and simulated (right column) normalized intensity distributions at distances z behind the second lens, color-coded in a linear scale. The white lines represent the semi-axes. The parameters of the setup are listed in Table 1. In the simulation, fitted parameters were used. At $z = 11.5$ cm the measured intensity ellipse angle with respect to the global y axis $\varphi_w^m = 69.3°$, and the angle of simulated intensity ellipse is $\varphi_w^s = 69°$. At $z = 14$ cm $\varphi_w^m = 73.5°$, and $\varphi_w^s = 73.6°$. At $z = 16$ cm $\varphi_w^m = 77.5°$, and $\varphi_w^s = 77.4°$.

6. Conclusion

The general astigmatic Gaussian beam as a general case of the Gaussian beam in the fundamental mode has been discussed. Such a beam can be fully described by three complex-valued parameters (q-parameters q_1, q_2 and complex-valued angle θ) or by the complex radius of curvature tensor Q [Eq. (7)]. The propagation law for a general astigmatic beam [Eq. (11)] is identical to that of the simple astigmatic beam. Alternatively, it can be represented using the complex radius of curvature tensor [Eq. (9)]. The real-valued parameters of the Gaussian beam in the fundamental mode can be obtained using Eqs. (24), (25) and eigenvalue computation from matrices $W(z)$ and $C(z)$ [Eq. (20)]. The transformation of the general astigmatic Gaussian beam at an arbitrary curved surface can be performed using Eqs. (55), (56) for the complex radius of curvature tensor. Altogether, it makes up a complete model for the description, propagation, and transformation of an arbitrary Gaussian beam in the fundamental mode. The suggested model is not restricted to nearly normal incidence and aligned optical systems. It can be used in the optical simulations of a large variety of 3D optical systems and in signal computation. The experimental verification of the evolution of the intensity distribution of the general astigmatic beam proved the reliability of the model.

References

1. H. Kogelnik and T. Li, "Laser beams and resonators," Appl. Opt. **5**, 1550–1567 (1966).
2. J. Alda, "Laser and Gaussian beam propagation and transformation," in *Encyclopedia of Optical Engineering* (Marcel Dekker, 2003), pp. 999–1013.
3. G. A. Massey and A. E. Siegman, "Reflection and refraction of Gaussian light beams at tilted ellipsoidal surfaces," Appl. Opt. **8**, 975–978 (1969).
4. J. A. Arnaud and H. Kogelnik, "Gaussian light beams with general astigmatism," Appl. Opt. **8**, 1687–1694 (1969).
5. A. Rohani, A. A. Shishegar, and S. Safavi-Naeini, "A fast Gaussian beam tracing method for reflection and refraction of general vectorial astigmatic Gaussian beams from general curved surfaces," Opt. Commun. **232**, 1–10 (2004).
6. E. Kochkina, G. Heinzel, G. Wanner, V. Müller, C. Mahrdt, B. Sheard, S. Schuster, and K. Danzmann, "Simulating and optimizing laser interferometers," in *9th LISA Symposium, Paris,* ASP Conference Series (Astronomical Society of the Pacific, 2013), vol. **467**, pp. 291–292.
7. G. Wanner, G. Heinzel, E. Kochkina, C. Mahrdt, B. Sheard, S. Schuster, and K. Danzmann, "Methods for simulating the readout of lengths and angles in laser interferometers with Gaussian beams," Opt. Commun. **285**, 4831–4839 (2012).
8. J. Alda, S. Wang, and E. Bernabeu, "Analytical expression for the complex radius of curvature tensor Q for generalized Gaussian beams," Opt. Commun. **80**, 350–352 (1991).
9. A. E. Siegman, *Lasers* (University Science, 1986), pp. 626–697.
10. A. B. Plachenov, V. N. Kudashov, and A. M. Radin, "Simple formula for a Gaussian beam with general astigmatism in a homogeneous medium," Opt. Spectrosc. **106**, 910–912 (2009).
11. J. Serna and G. Nemes, "Decoupling of coherent Gaussian beams with general astigmatism," Opt. Lett. **18**, 1774–1776 (1993).
12. G. A. Deschamps, "Ray techniques in electromagnetics," Proc. IEEE **60**, 1022–1035 (1972).
13. G. J. James, *Geometrical Theory of Diffraction for Electromagnetic Waves*, 3rd ed. (Peter Peregrinus, 1986), pp. 96–116.
14. E. Hecht, *Optics* (Addison-Wesley, 1974), pp. 60–98.